Electronic Supplementary Material (ESI) for Inorganic Chemistry Frontiers.

Supporting Information

A Fluorine-functionalized Microporous In-MOF with High Physicochemical Stability for Light Hydrocarbon Storage and Separation

Weidong Fan, † Xiuping Liu, † Xia Wang, Yue Li, Chengyong Xing, Yutong Wang, Wenyue Guo, Liangliang Zhang, and Daofeng Sun*

State Key Laboratory of Heavy Oil Processing, College of Science, China University of Petroleum (East China), Qingdao, Shandong 266580, People's Republic of China.

Email: dfsun@upc.edu.cn.

Table of Contents

1. Synthesis of H_3TTCA-F

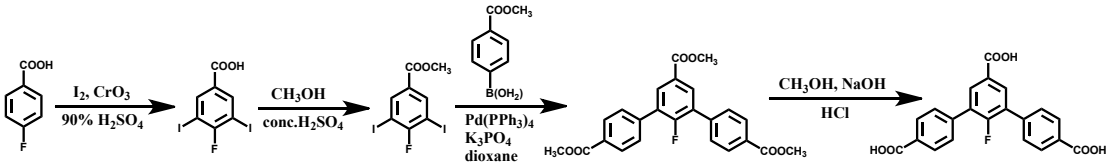

Scheme S1. Synthetic procedures of the H_3TTCA-F ligand.

(1) 4-fluoro-3,5-diiodobenzoic acid

According to literature,[1] to finely powdered iodine (5.08 g, 20.0mmol) suspended in H_2SO_4(90%, 100ml, V/V) was added CrO_3 (2.0g, 20.0 mmol). The mixture was stirred at about 30℃ for 30 min. To the solution was added 4-fluorobenzoic acid (2.10 g, 15.0 mmol). The mixture was stirred at 25-30℃ for 24 h and then poured into ice/water and filtered by a vacuum. The solid was washed with cool water and then dried by vacuum at 50 ℃. Crude (3.41 g, 58%) as a white solid which was used without further purification.

(2) Methyl 4-fluoro-3,5-diiodobenzoate

A sample of 4-fluoro-3,5-diiodobenzoic acid (19.6 g, 50.0 mmol) was suspended in 200 ml of absolute methanol at room temperature. Concentrated H_2SO_4 (9.5ml) was added slowly with rapid stirring and then the reaction mixture was heated at reflux for 48 h. At the end of the reflux period, TLC (silica, CH_2Cl_2) indicated the complete consumption of the starting material. The solution was initially cooled to room temperature, and then in an ice bath to precipitate the product. Vacuum filtration afforded 18.87 g (93%) of a white solid. ^{1}H NMR (400 MHz, $CDCl_3$) 3.88 (s, 3 H), 8.32 (s, 2 H). Anal. Calcd. for $C_8H_5I_2FO_2$ (mw 406): C, 23.65; H, 1.23. Found: C, 23.63; H, 1.21.

(3) Trimethyl 2'-fluoro-[1,1':3',1''-terphenyl]-4,4'',5'-tricarboxylate

Methyl 4-fluoro-3,5-diiodobenzoate (1.62 g, 4 mmol), Methyl 4-boronobenzoate (1.57 g, 9.6 mmol), $Pd(PPh_3)_4$ (0.15 g, 0.13 mmol) and K_3PO_4 (3.82 g, 18.0 mmol) were placed in a 500 ml two-necked round bottom flask under a N_2 gas atmosphere. The flask was further charged with a 200 mL of dry 1,4-dioxane, and the contents were heated for 48 h. After the mixture was cooled to room temperature, the solvent was removed, water was added. The water phase was washed with CH_2Cl_2. The mixed organic phases were dried with $MgSO_4$. After the solvent was removed, the crude product was purified by column chromatography with CH_2Cl_2 as the eluent. ^1H NMR (400 MHz, $CDCl_3$) 3.87(s, 3H), 3.96(s, 6H), 7.81(d, 4H), 8.16(s, 2H), 8.29(d, 4H). Anal. Calcd. for $C_{24}H_{19}FO_6$ (mw 422): C, 68.25; H, 4.50. Found: C, 68.27; H, 4.55.

(4) 2'-fluoro-[1,1':3',1''-terphenyl]-4,4'',5'-tricarboxylic acid

Trimethyl 2'-fluoro-[1,1':3',1''-terphenyl]-4,4'',5'-tricarboxylate (2.0 g, 4.7 mmol) was dissolved in 50 ml MeOH, 50 ml 2 M NaOH aqueous solution was added. The mixture was stirred at 50 ℃ overnight. The organic phase was removed, the aqueous phase was acidified with diluted hydrochloric acid to give yellow precipitate, which was filtered and wased with water several times. ^1H NMR (400 MHz, $CDCl_3$) 7.66(d, 4H), 7.94(s, 2H), 8.06(d, 4H), 12.78(s, 3H). Anal. Calcd. for $C_{21}H_{15}NO_6$ (mw 377): C, 66.84; N, 3.71; H, 4.01. Found: C, 66.78; N, 3.73; H, 4.00.

2. Synthesis of UPC-104.

A mixture of H_3TTCA-F (10.0 mg, 0.026 mmol) and $In(NO_3)_3 \cdot 4.5H_2O$ (15.0 mg, 0.04 mmol) were ultrasonically dissolved in DMF (2 mL) solution in 10 mL vial, then 6d of HNO_3 (1:5) was added. The mixtures were slowly heated to 115 °C from room temperature in 5 hours, then kept at 115 °C for 2 days. After slowly cooled to 30 °C in 10 hours, the colourless block crystals were separated in 37% yield based on H_3TTCA-F. Phase purity of the crystals was confirmed by powder X-ray diffraction (PXRD). FT-IR (KBr, cm^{-1}): 3401(w), 3069(w), 1658 (s), 1597(s), 1549(w), 1407(s), 1317(w), 1253(w), 1217(w), 1181(w), 1099(m), 1019(m), 870(m), 784(s), 724(s); elemental analysis (EA, %) calculated for $\{[In_{1.5}(\mu_3\text{-}O)(F\text{-}TPTA)(Me_2NH_2)(H_2O)] \cdot 4DMF \cdot 3H_2O\}$: C, 43.05; H, 5.54; N, 7.18; found: C, 43.12; H, 5.49; N, 7.10.

2. Crystal data, structure and characterization of UPC-104.

Table S1. Crystal data and structure refinement of **UPC-104** with CCDC 1837588.

Identification code	**UPC-104**
Empirical formula	$C_{20.5}H_{11.83}FIn_{1.5}O_{7.67}$
Formula weight	572.03
Temperature/K	150.01(10)
Crystal system	trigonal
Space group	R-3c
a/Å	27.3963(13)
b/Å	27.3963(13)
c/Å	75.861(3)
α/°	90
β/°	90
γ/°	120
Volume/Å^3	49310(5)
Z	36
ϱ_{calc} mg/mm^3	0.693
μ/mm^{-1}	5.270
F(000)	10032.0
2Θ range for data collection	7.34 to 141.558°
Reflections collected	37141
Independent reflections	10368 [Rint = 0.0475, Rsigma = 0.0732]
Data/restraints/parameters	10368/0/288
Goodness-of-fit on F^2	1.093
Final R indexes [I>=2σ (I)]	R1 = 0.0843, wR2 = 0.2675
Final R indexes [all data]	R1 = 0.1080, wR2 = 0.2991
Largest diff. peak/hole /e Å$^-$	1.37/-1.16

Table S2. Selected bond lengths (Å) and selected bond angles (º) for **UPC-104**.

Atom	Atom	Length/Å	Atom	Atom	Atom	Angle/°	Atom	Atom	Atom	Angle/°
In1	O4	2.176(6)	O4	In1	$O5^{1}$	169.3(3)	$O3^{2}$	In1	O4	90.2(3)
In1	O30	2.136(8)	O30	In1	O4	84.7(3)	$O3^{2}$	In1	$O5^{1}$	93.7(3)
In1	O1	2.040(4)	O30	In1	$O5^{1}$	85.7(3)	O6	In2	$O6^{4}$	171.2(4)
In1	$O2^{1}$	2.130(6)	O1	In1	O4	96.7(2)	O6	In2	O8	85.6(2)
In1	$O5^{2}$	2.194(7)	O1	In1	O30	177.7(3)	O6	In2	$O7^{5}$	92.5(4)
In1	$O3^{3}$	2.153(7)	O1	In1	$O2^{3}$	94.9(2)	O1	In2	O6	94.4(2)
In2	O6	2.124(6)	O1	In1	$O5^{1}$	93.0(2)	O1	In2	O8	180.0
In2	$O6^{4}$	2.124(6)	O1	In1	$O3^{2}$	92.4(3)	O1	In2	$O7^{5}$	92.0(3)
In2	O1	2.025(8)	$O2^{3}$	In1	O4	85.7(3)	O1	In2	$O7^{2}$	92.0(3)
In2	O8	2.199(12)	$O2^{3}$	In1	O30	87.0(4)	$O7^{2}$	In2	O8	88.0(3)
In2	$O7^{3}$	2.182(9)	$O2^{3}$	In1	$O5^{1}$	89.2(3)	$O7^{5}$	In2	O8	88.0(3)
In2	$O7^{5}$	2.182(9)	$O2^{3}$	In1	$O3^{2}$	172.0(3)	$O7^{5}$	In2	$O7^{2}$	176.0(6)

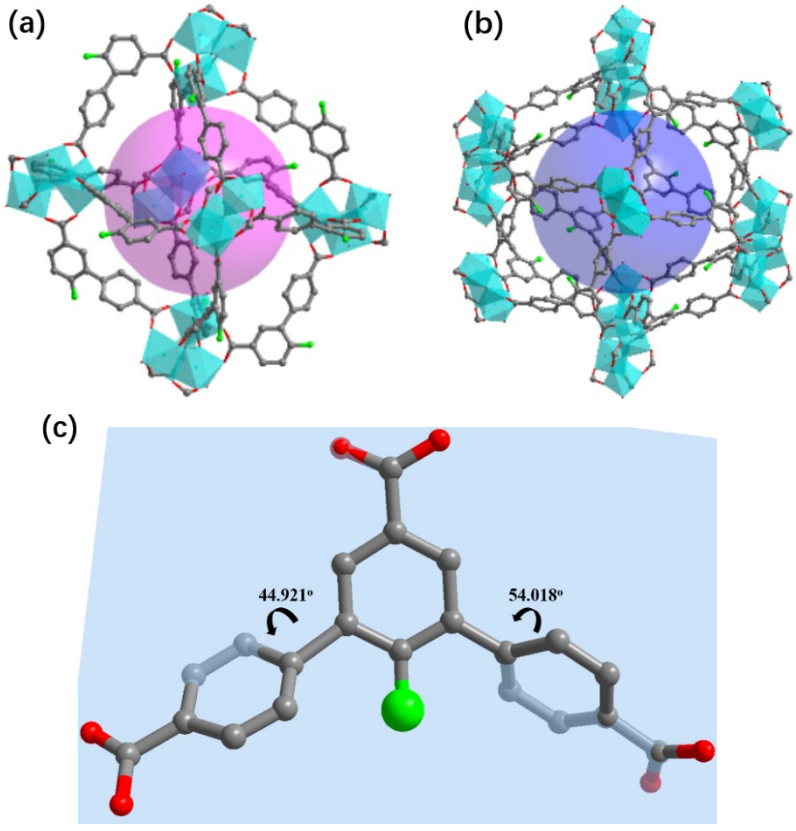

Figure S1. (a,b)The prime network of **UPC-104** consists of two different types of hollow cages. (c) The dihedral angles between two sloping pendant benzene groups and the central benzene ring in TTCA-F for **UPC-104**.

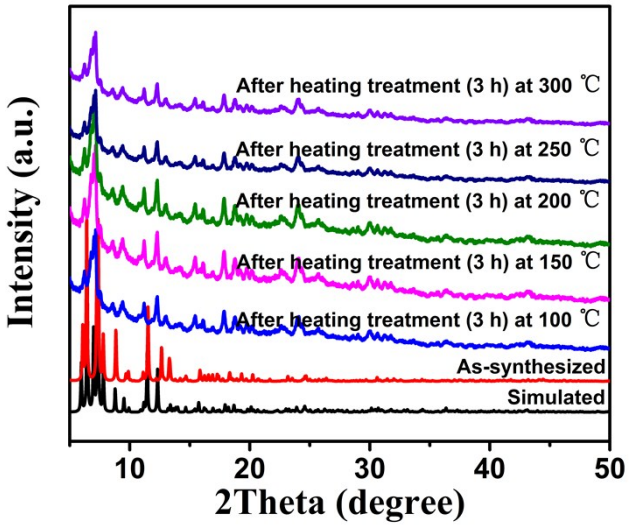

Figure S2. Powder X-ray diffraction (PXRD) of **UPC-104** under different temperatures.

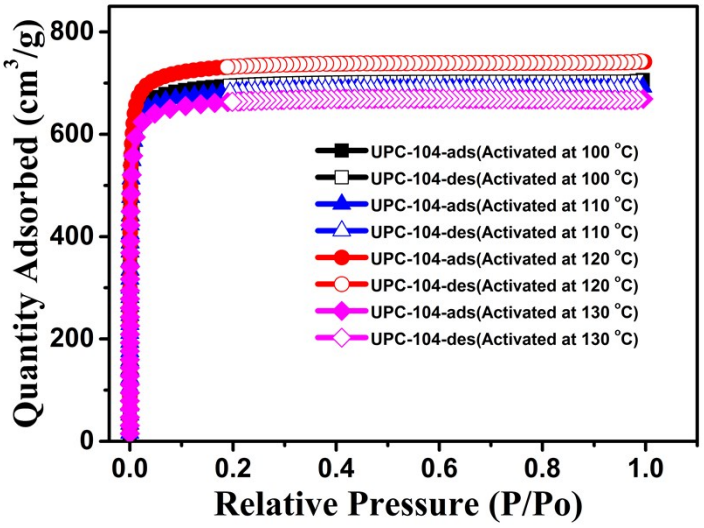

Figure S3. N_2 sorption isotherms at different activation temperatures of **UPC-104**.

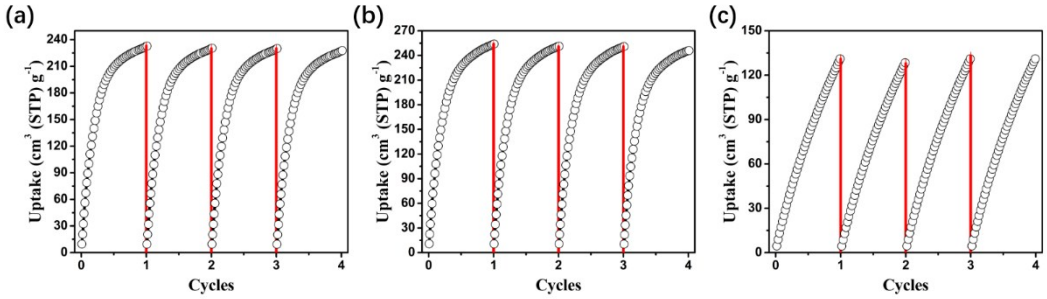

Figure S4. Cycles of C_3H_8 (a), C_3H_6 (b) and C_2H_2 (c) adsorption for **UPC-104** at 298 K.

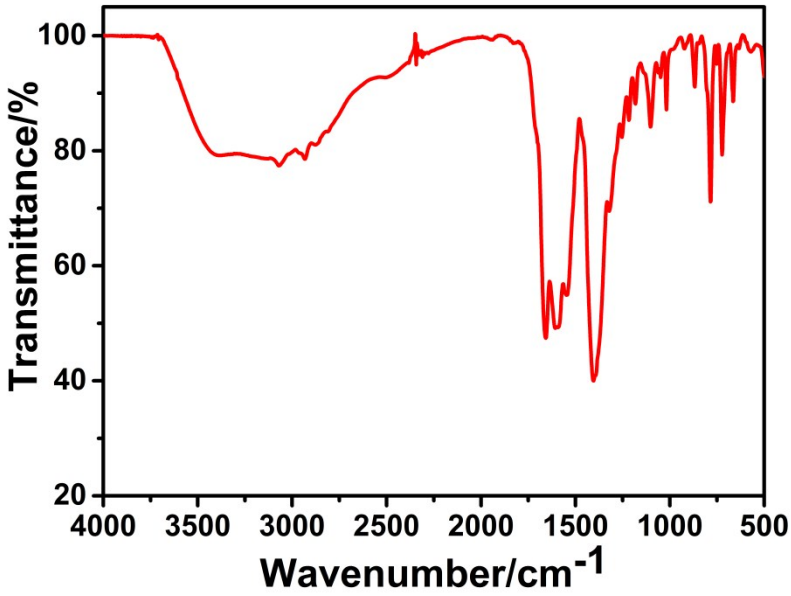

Figure S5. The IR of **UPC-104**.

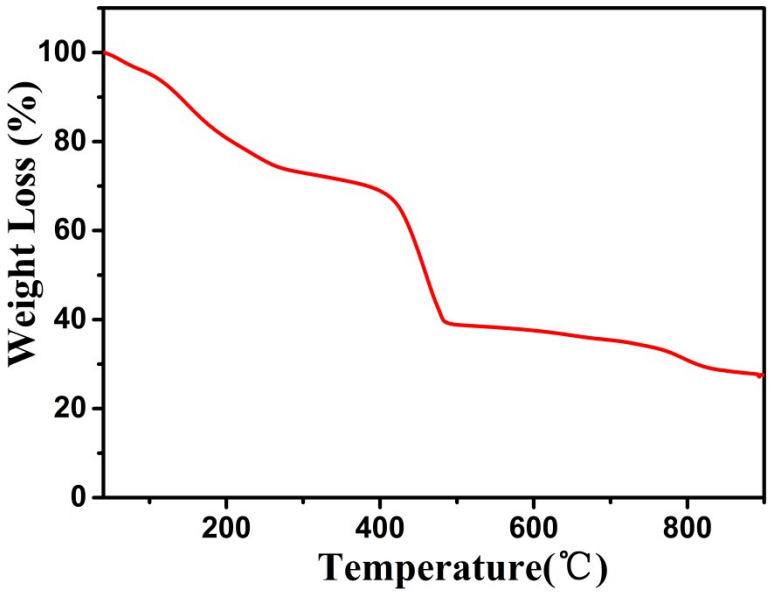

Figure S6. The TGA of **UPC-104**.

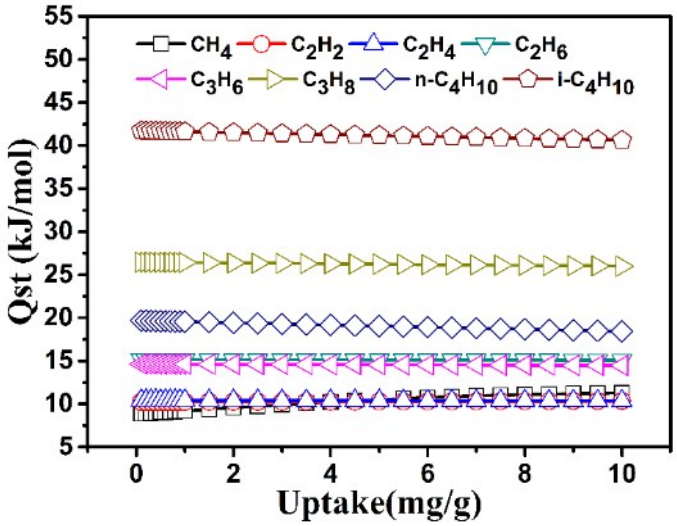

Figure S7. The *Q*st for CH_4, C_2H_2, C_2H_4, C_2H_6, C_3H_6, C_3H_8 , n-C_4H_{10}, and i-C_4H_{10} for **UPC-104**.

3. Hydrogen and light hydrocarbon adsorption of UPC-104.

Table S3. Single component gas adsorption Data for **UPC-104.**

Gas	T [K]		Vads [$cm^3 \cdot g^{-1}$]	Amount [$mmol \cdot g^{-1}$] [wt%]	Qst [$KJ \cdot mol^{-1}$]
CH_4	273	26.6	1.19	1.90	8.8
	298	18.1	0.81	1.30	
C_2H_2	273	187.0	8.35	21.71	10.3
	298	131.0	5.85	15.21	
C_2H_4	273	139.1	6.21	17.39	10.4
	298	108.7	4.85	13.59	
C_2H_6	273	180.6	8.06	24.18	15.1
	298	133.8	5.97	17.92	
C_3H_6	273	276.5	12.34	51.84	14.6
	298	253.9	11.33	47.61	
C_3H_8	273	250.4	11.18	49.19	26.5
	298	232.8	10.39	45.73	
n-C_4H_{10}	273	176.1	7.86	45.60	19.7
	298	165.1	7.37	42.75	
i-C_4H_{10}	273	178.8	7.98	46.30	41.7
	298	164.8	7.36	42.67	

Table S4. UPC-104: adsorption selectivity of hydrocarbon at 1 bar for different molar fraction of binary mixtures.

binary gas mixtures	molar fraction	Selectivity (273K)	Selectivity (298K)
C_2H_2/CH_4	50:50	12.0	11.8
	10:90	11.6	11.7
C_2H_4/CH_4	50:50	8.5	8.9
	10:90	8.4	8.7
C_2H_6/CH_4	50:50	14.3	12.3
	10:90	13.9	12.0
C_3H_6/CH_4	50:50	122.5	97.9
	10:90	83.7	71.1
C_3H_8/CH_4	50:50	126.9	79.0
	10:90	99.6	58.0
n-C_4H_{10}/CH_4	50:50	26.1	28.5
	10:90	19.7	19.9
i-C_4H_{10}/CH_4	50:50	241.5	163.7

	10:90	327.0	212.2

Table S5. Comparison of H_2 Adsorption Data for Selected MOFs.

	H_2 uptake (77K, 1bar, wt%)	ref		H_2 uptake (wt%)	ref
UPC-104	**2.06**	**This work**	SNU-1	1.90	11
NOTT-400	2.14	2	SNU-77H	1.79	12
CUK-1	1.6	3	FJI-1	1.02	13
SNU-5	1.83	4	MOF-74(Mg)	2.2	14
SNU-6	1.68	5	PCN-9	1.53	15
ZIF-8	1.27	6	PCN-6	1.9	16
ZIF-11	1.35	6	PCN-6′	1.35	17
SNU-4	2.07	7	UMCM-150	2.1	18
MOF-646	1.75	8	TUDMOF-1	1.75	19
MOF-5	1.32	9	PCN-21	1.6	20
MOF-177	1.25	9	PCN-46	1.95	21
IRMOF-11	1.62	9	SNU-21S	1.95	22
IRMOF-8	1.50	9	SNU-21H	1.64	22
IRMOF-9	1.17	10	SNU-50′	2.1	23
IRMOF-2	1.21	10	PCN-61	2.25	24
IRMOF-6	1.48	10	PCN-66	1.79	24
IRMOF-3	1.42	10	PCN-68	1.87	24
IRMOF-20	1.35	10	NOTT-119	1.4	25
IRMOF-13	1.73	10	PCN-69	1.7	26
MOF-74(Zn)	1.77	10	NU-100	1.82	27

Table S6. Comparison of gas sorptions with C_2H_2 for selected MOF.

Materials	C_2H_2 uptake ($cm^3\ g^{-1}$)	ref	Materials	C_2H_2 uptake ($cm^3\ g^{-1}$)	ref
UPC-104	**187**	**This work**	1-Cu_2(bpz)	58	51
ZJU-26	84	28	1-Ag_2(bpz)	44	51
Cu-TDPAT	155.7	29	Cu(etz)	70	52
ZJU-40a	216	30	MOF-505	148	53
NOTT-101a	184	30	MOF-508	90	53
MOF-1	100	31	MIL-53	72	53
MOF-2	31	31	MOF-5	26	53
PCP-33	121.8	32	ZIF-8	25	53
UTSA-74	145	33	CoMOF-74	197	54
UTSA-68a	70.1	33	MnMOF-74	168	54
UTSA-50a	90.6	34	MgMOF-74	184	54
HKUST-1	201	35	ZnMOF-74	122	54
ZJNU-47a	214	36	FeMOF-74	156	55
ZJNU-61	48	37	UMCM-150	129	56
ZJU-30a	52.6	38	PCN-16	176	56
ZJU-199	128	39	NOTT-101	184	56
ZJU-72a	167.7	40	NOTT-102	146	56
UTSA-5a	59.8	41	UTSA-20	150	56
MMOF-20a	21	42	UTSA-33a	84	57
FJI-C4	72.5	43	UTSA-34b	121	58
UTSA-72a	27.8	44	UTSA-35a	65	59
ZJU-10a	174	45	UTSA-36a	57	60
FJU-C1	93.8	46	UTSA-38a	64	61
BUT-70A	69.5	47	Cu_2(ebtc)	160	62
BUT-70B	87.1	47	$Zn_5(bta)_6(tda)_2$	44	63
$Cu_2(pzdc)_2(pyz)$	42	48	$Zn_4(OH)_2(1,2,4\text{-btc})_2$	53	64
$Mg(HCO_2)_2$	66	49	Cu(bdc-OH)(4,40-bpy)	35	65
$Mn(HCO_2)_2$	51	49	Cu(bdc-OH)	43	66
$Cu_2(bdc)_2$(dabco)	60	50	Cu_4L^g	154	67
$Cu_2(ndc)_2$(dabco)	97	50	Yb(bpt)	24	68
$Cu_2(adc)_2$(dabco)	82	50	HOF-3a	47	69
$Zn_2(bdc)_2$(dabco)	93	50	UPC-21	196.5	70
$Zn_2(ndc)_2$(dabco)	106	50	UPC-33	65.1	71
$Zn_2(adc)_2$(dabco)	101	50	UPC-30	30.9	72

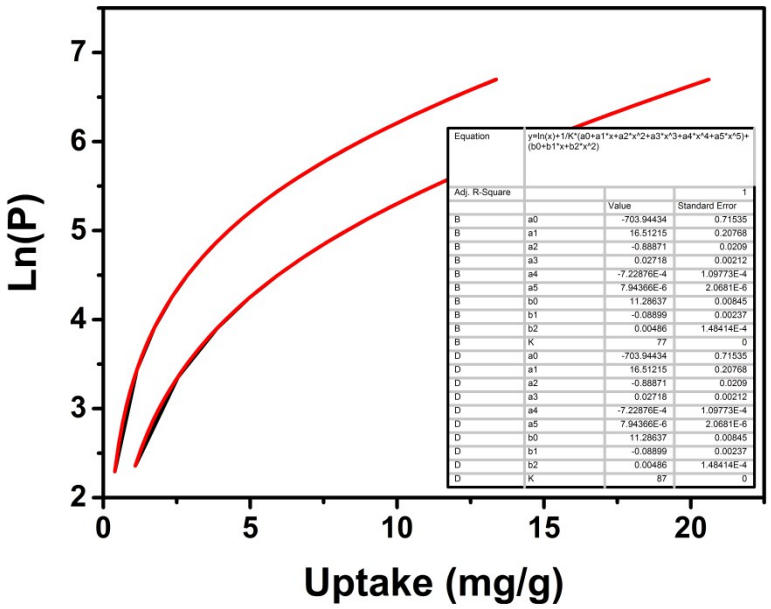

Figure S8. UPC-104: the parameters and optimized adsorption isotherms for calculated Q_{st} of H_2 using a variant of the Clausius-Clapeyron equation.

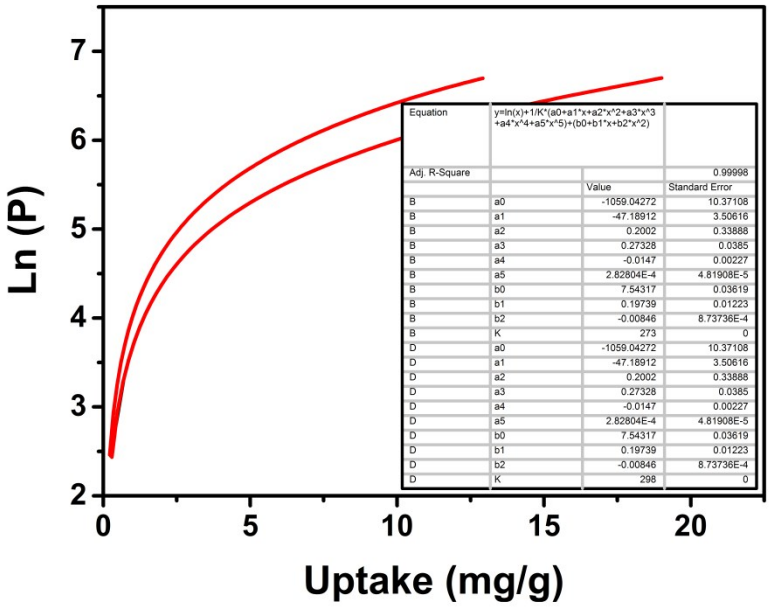

Figure S9. UPC-104: the parameters and optimized adsorption isotherms for calculated Q_{st} of CH_4 using a variant of the Clausius-Clapeyron equation.

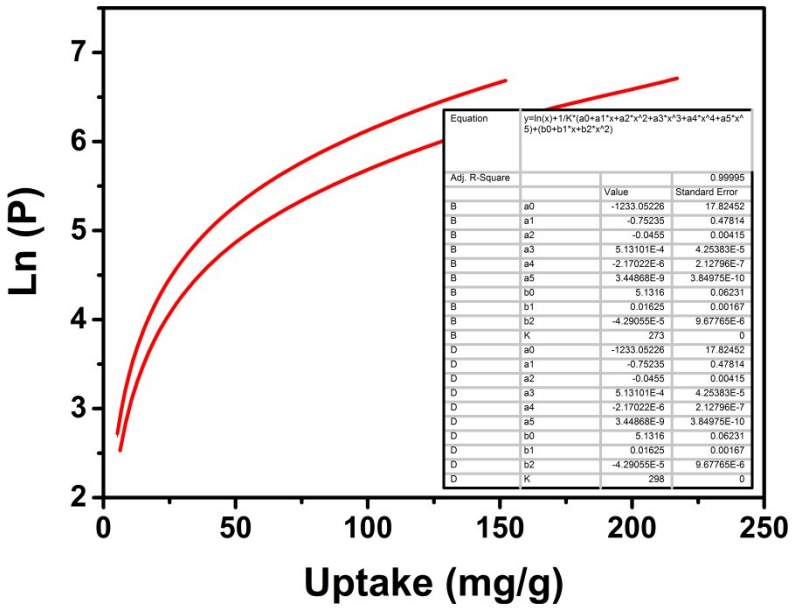

Figure S10. UPC-104: the parameters and optimized adsorption isotherms for calculated Q_{st} of C_2H_2 using a variant of the Clausius-Clapeyron equation.

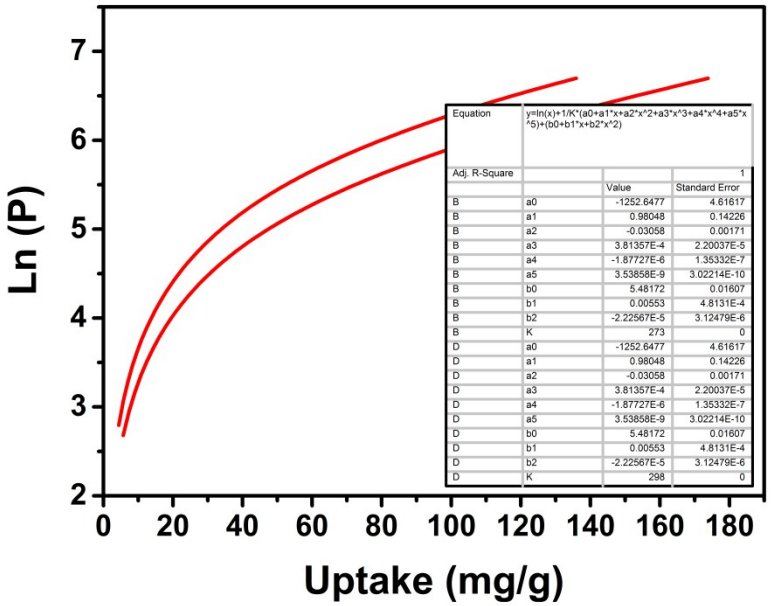

Figure S11. UPC-104: the parameters and optimized adsorption isotherms for calculated Q_{st} of C_2H_4 using a variant of the Clausius-Clapeyron equation.

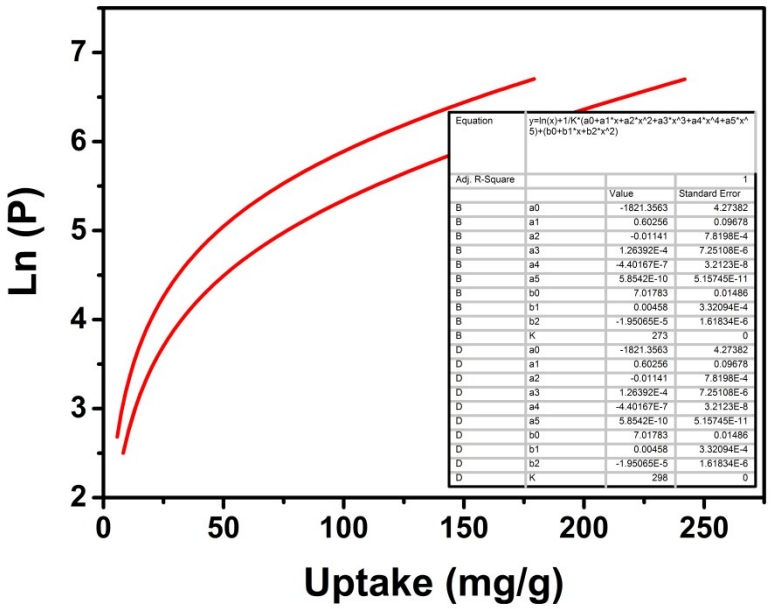

Equation	y=ln(x)+1/K*(a0+a1*x+a2*x^2+a3*x^3+a4*x^4+a5*x^5)+(b0+b1*x+b2*x^2)		
Adj. R-Square			1
		Value	Standard Error
B	a0	-1821.3563	4.27382
B	a1	0.60256	0.09678
B	a2	-0.01141	7.8198E-4
B	a3	1.26392E-4	7.25108E-6
B	a4	-4.40167E-7	3.2123E-8
B	a5	5.8542E-10	5.15745E-11
B	b0	7.01783	0.01486
B	b1	0.00458	3.32094E-4
B	b2	-1.95065E-5	1.61834E-6
B	K	273	0
D	a0	-1821.3563	4.27382
D	a1	0.60256	0.09678
D	a2	-0.01141	7.8198E-4
D	a3	1.26392E-4	7.25108E-6
D	a4	-4.40167E-7	3.2123E-8
D	a5	5.8542E-10	5.15745E-11
D	b0	7.01783	0.01486
D	b1	0.00458	3.32094E-4
D	b2	-1.95065E-5	1.61834E-6
D	K	298	0

Figure S12. UPC-104: the parameters and optimized adsorption isotherms for calculated Q_{st} of C_2H_6 using a variant of the Clausius-Clapeyron equation.

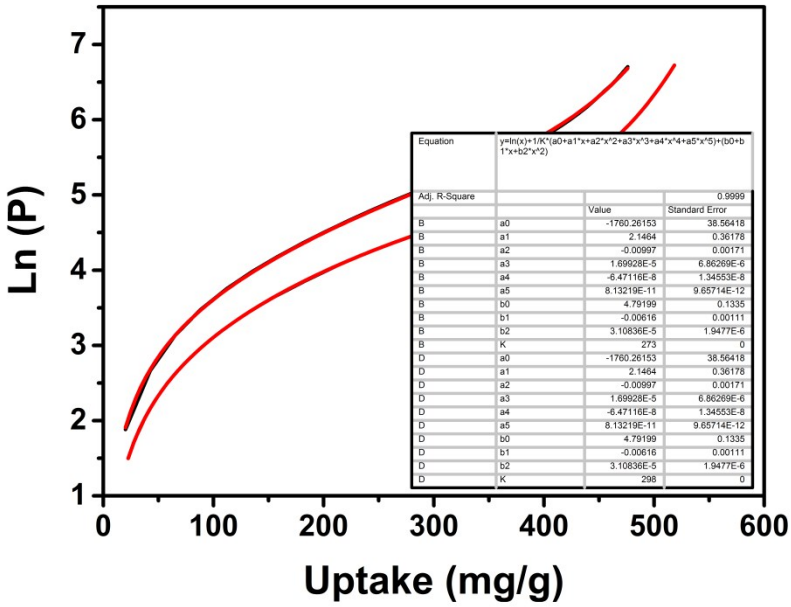

Equation	y=ln(x)+1/K*(a0+a1*x+a2*x^2+a3*x^3+a4*x^4+a5*x^5)+(b0+b1*x+b2*x^2)		
Adj. R-Square			0.9999
		Value	Standard Error
B	a0	-1760.26153	38.56418
B	a1	2.1464	0.36178
B	a2	-0.00997	0.00171
B	a3	1.69928E-5	6.86269E-6
B	a4	-6.47116E-8	1.34553E-8
B	a5	8.13219E-11	9.65714E-12
B	b0	4.79199	0.1335
B	b1	-0.00616	0.00111
B	b2	3.10836E-5	1.9477E-6
B	K	273	0
D	a0	-1760.26153	38.56418
D	a1	2.1464	0.36178
D	a2	-0.00997	0.00171
D	a3	1.69928E-5	6.86269E-6
D	a4	-6.47116E-8	1.34553E-8
D	a5	8.13219E-11	9.65714E-12
D	b0	4.79199	0.1335
D	b1	-0.00616	0.00111
D	b2	3.10836E-5	1.9477E-6
D	K	298	0

Figure S13. UPC-104: the parameters and optimized adsorption isotherms for calculated Q_{st} of C_3H_6 using a variant of the Clausius-Clapeyron equation.

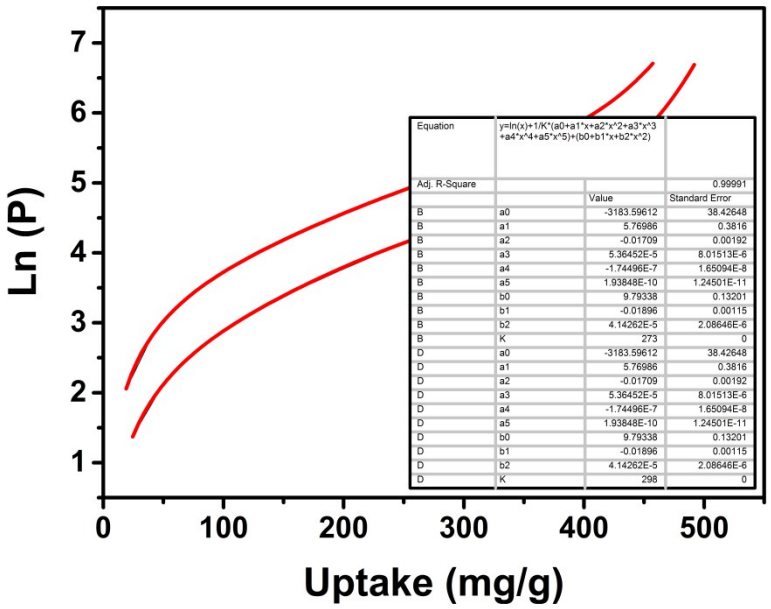

Figure S14. UPC-104: the parameters and optimized adsorption isotherms for calculated Q_{st} of C_3H_8 using a variant of the Clausius-Clapeyron equation.

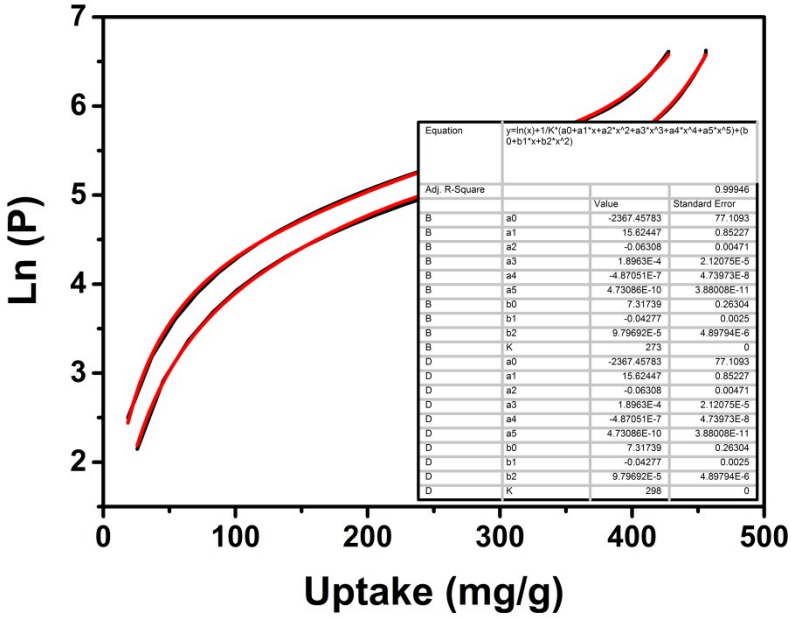

Figure S15. UPC-104: the parameters and optimized adsorption isotherms for calculated Q_{st} of n-C_4H_{10} using a variant of the Clausius-Clapeyron equation.

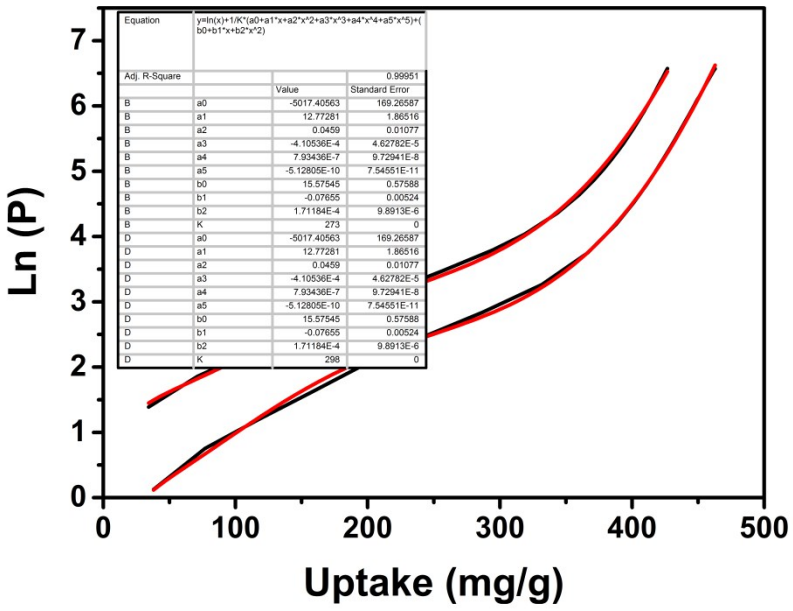

Figure S16. UPC-104: the parameters and optimized adsorption isotherms for calculated Q_{st} of i-C_4H_{10} using a variant of the Clausius-Clapeyron equation.

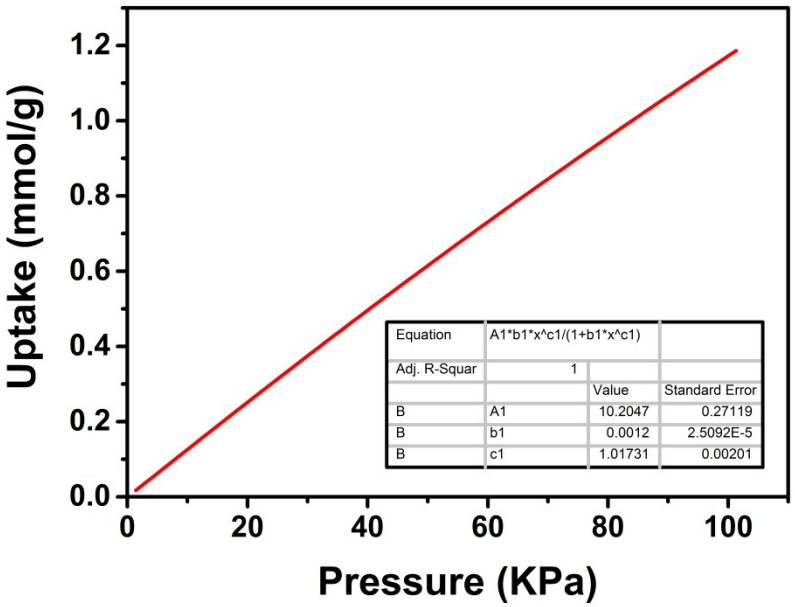

Figure S17. UPC-104: the parameters and optimized adsorption isotherms of CH_4 for calculated selectivity by using Ideal Adsorbed Solution Theory (IAST) at 273K.

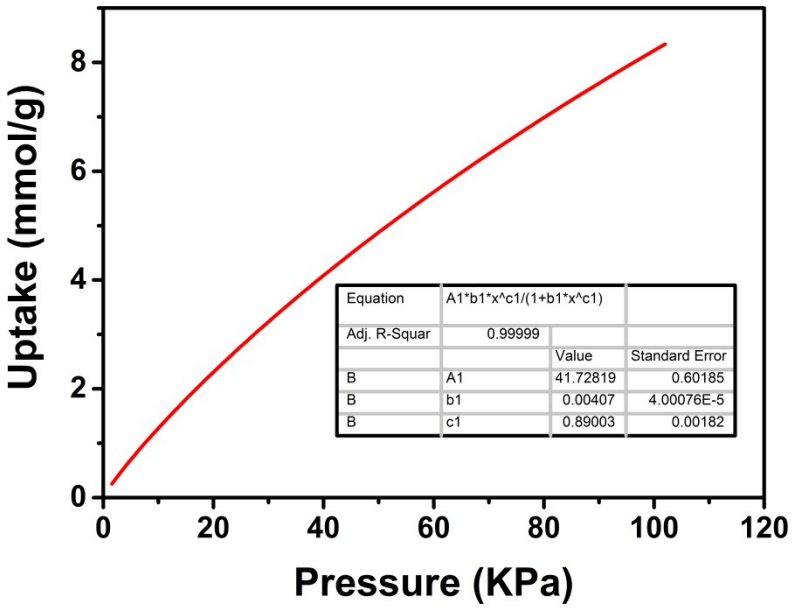

Figure S18. UPC-104: the parameters and optimized adsorption isotherms of C_2H_2 for calculated selectivity by using Ideal Adsorbed Solution Theory (IAST) at 273K.

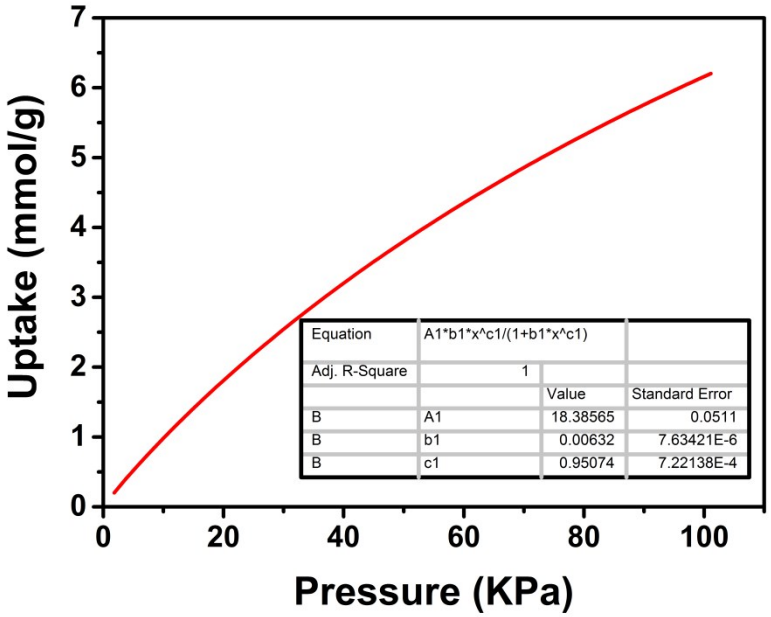

Figure S19. UPC-104: the parameters and optimized adsorption isotherms of C_2H_4 for calculated selectivity by using Ideal Adsorbed Solution Theory (IAST) at 273K.

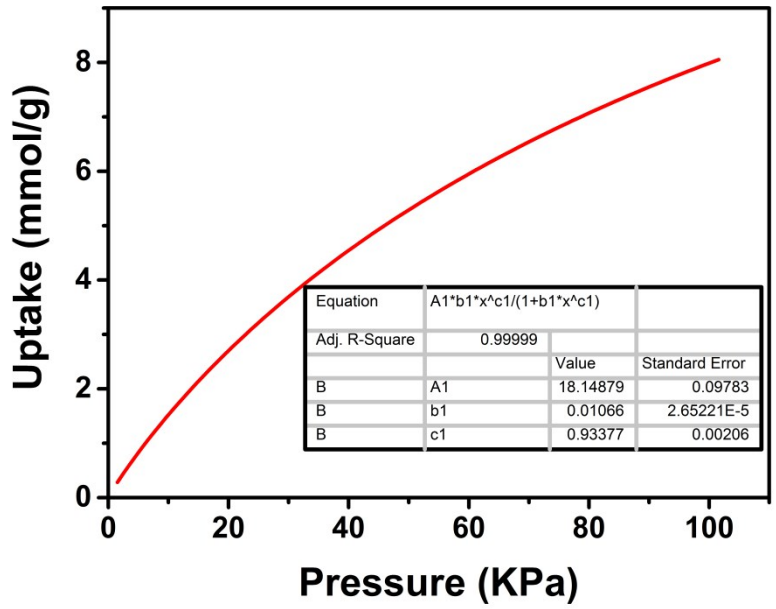

Figure S20. UPC-104: the parameters and optimized adsorption isotherms of C_2H_6 for calculated selectivity by using Ideal Adsorbed Solution Theory (IAST) at 273K.

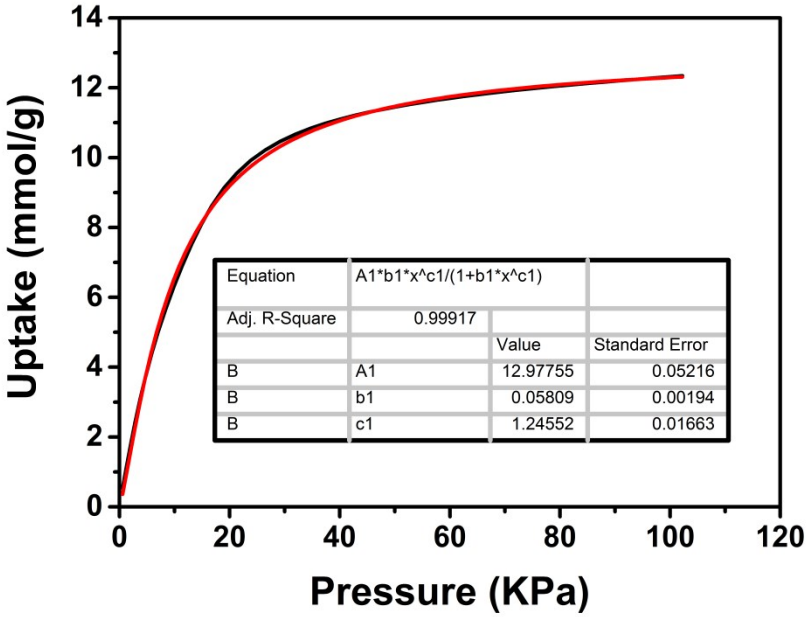

Figure S21. UPC-104: the parameters and optimized adsorption isotherms of C_3H_6 for calculated selectivity by using Ideal Adsorbed Solution Theory (IAST) at 273K.

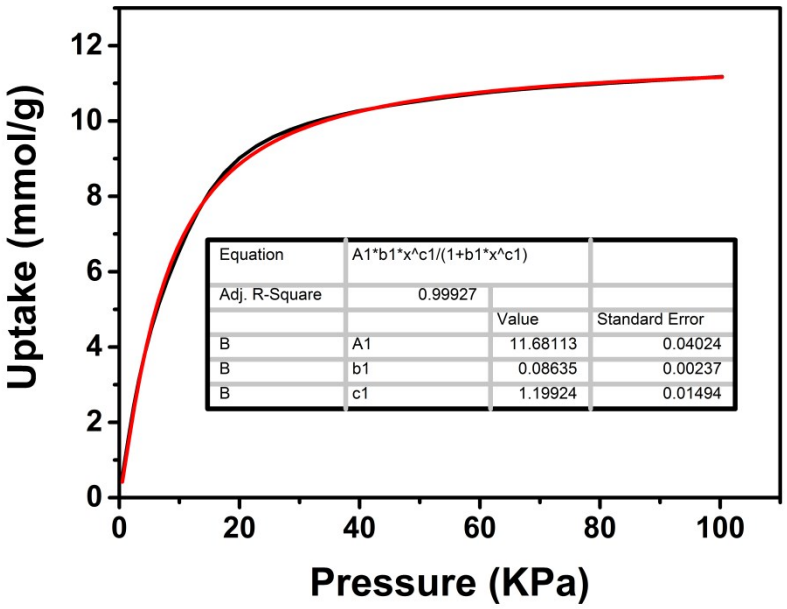

Figure S22. UPC-104: the parameters and optimized adsorption isotherms of C_3H_8 for calculated selectivity by using Ideal Adsorbed Solution Theory (IAST) at 273K.

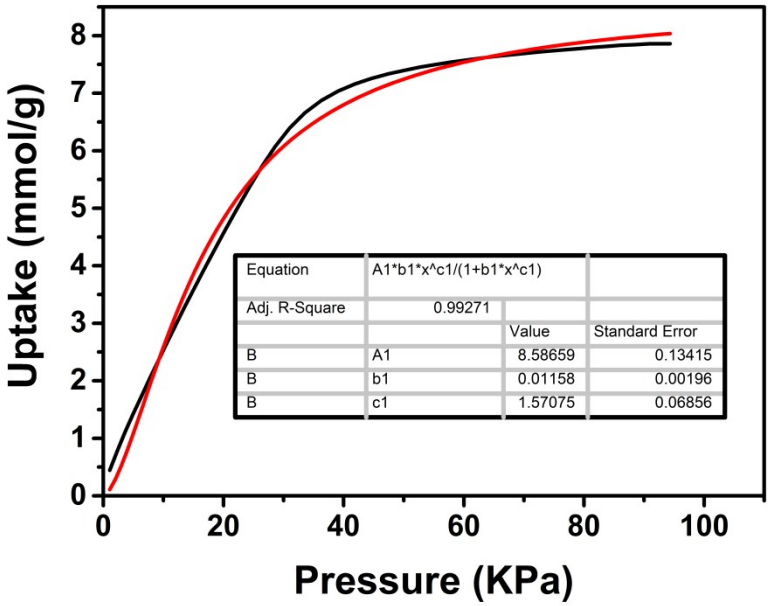

Figure S23. UPC-104: the parameters and optimized adsorption isotherms of n-C_4H_{10} for calculated selectivity by using Ideal Adsorbed Solution Theory (IAST) at 273K.

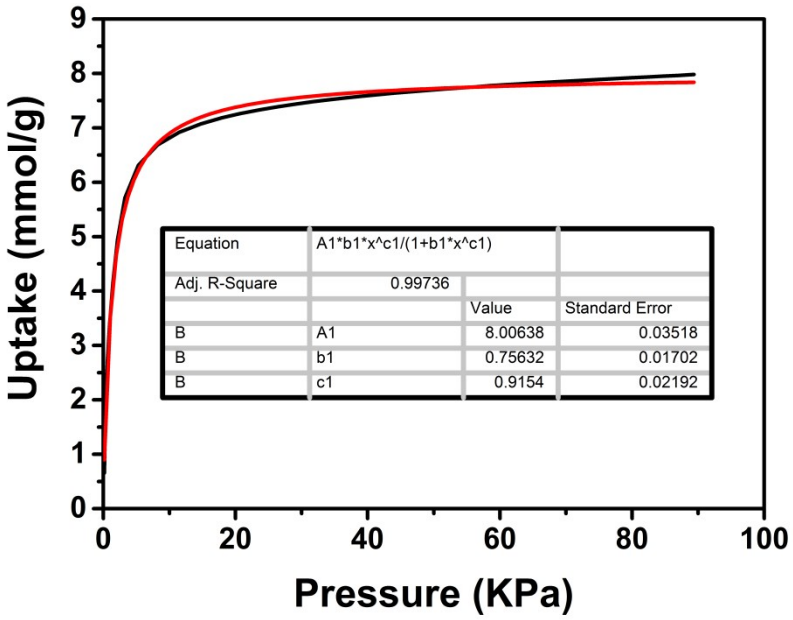

Figure S24. UPC-104: the parameters and optimized adsorption isotherms of i-C_4H_{10} for calculated selectivity by using Ideal Adsorbed Solution Theory (IAST) at 273K.

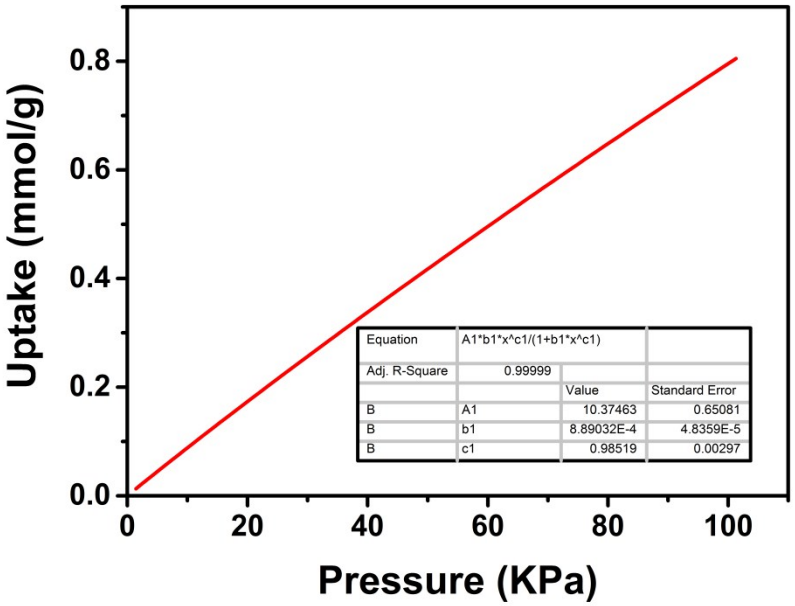

Figure S25. UPC-104: the parameters and optimized adsorption isotherms of CH_4 for calculated selectivity by using Ideal Adsorbed Solution Theory (IAST) at 298K.

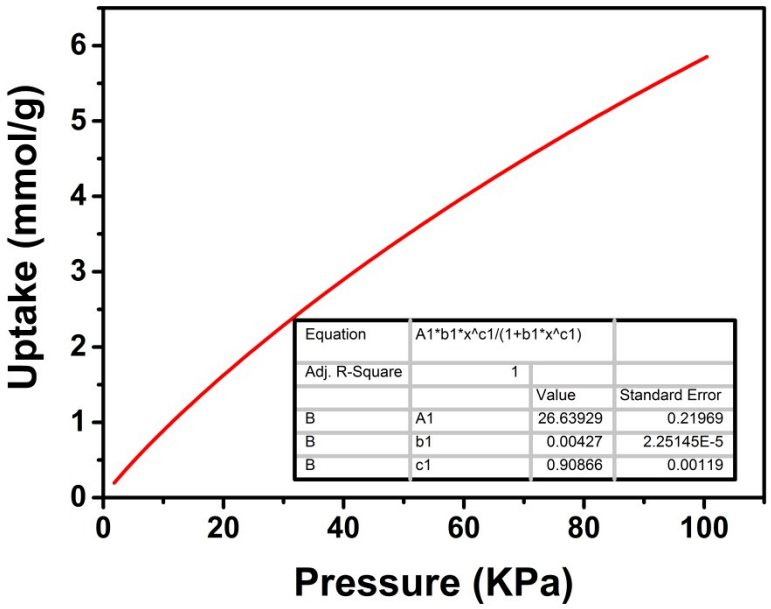

Figure S26. UPC-104: the parameters and optimized adsorption isotherms of C_2H_2 for calculated selectivity by using Ideal Adsorbed Solution Theory (IAST) at 298K.

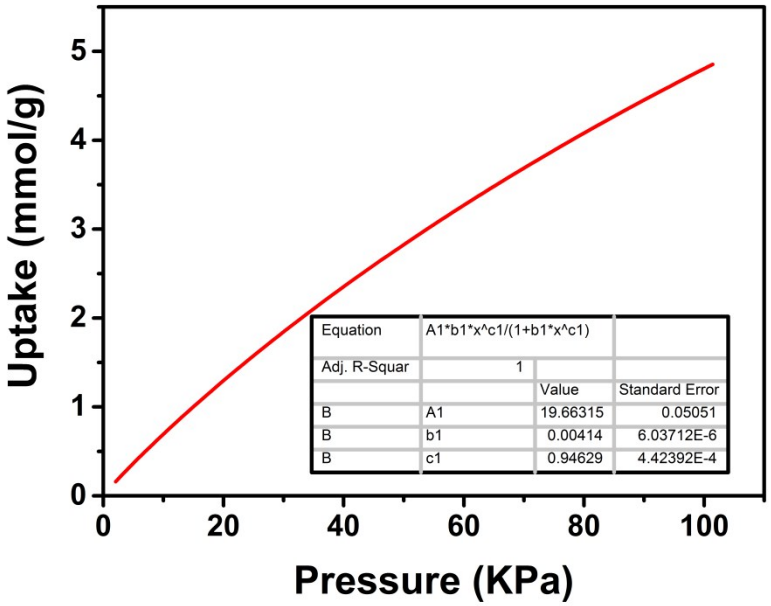

Figure S27. UPC-104: the parameters and optimized adsorption isotherms of C_2H_4 for calculated selectivity by using Ideal Adsorbed Solution Theory (IAST) at 298K.

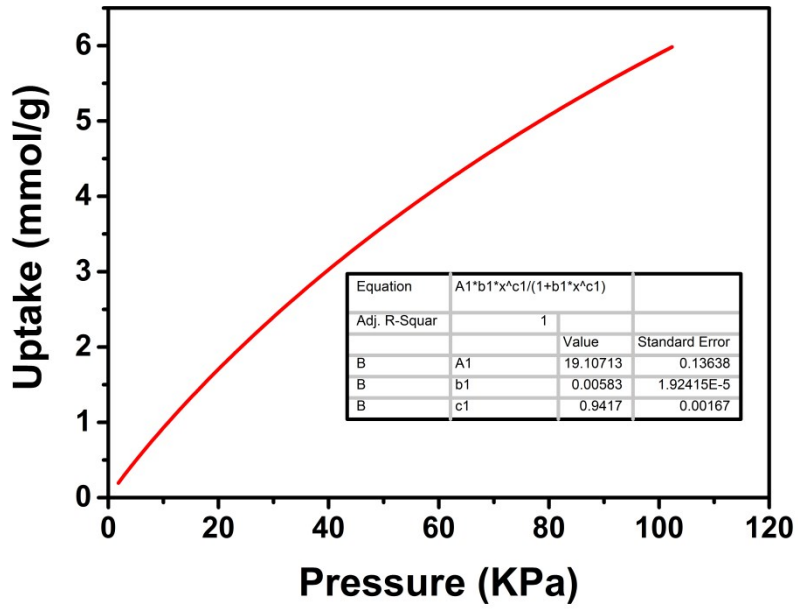

Figure S28. UPC-104: the parameters and optimized adsorption isotherms of C_2H_6 for calculated selectivity by using Ideal Adsorbed Solution Theory (IAST) at 298K.

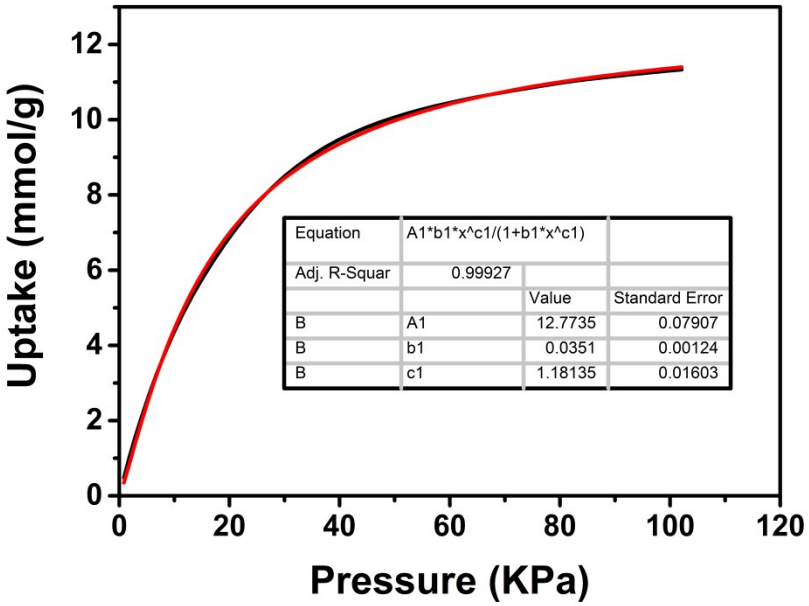

Figure S29. UPC-104: the parameters and optimized adsorption isotherms of C_3H_6 for calculated selectivity by using Ideal Adsorbed Solution Theory (IAST) at 298K.

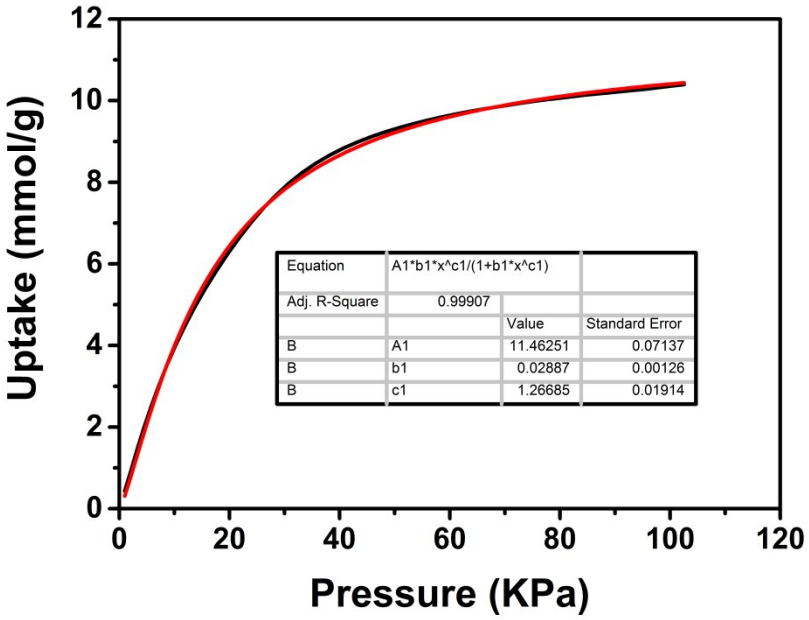

Figure S30. UPC-104: the parameters and optimized adsorption isotherms of C_3H_8 for calculated selectivity by using Ideal Adsorbed Solution Theory (IAST) at 298K.

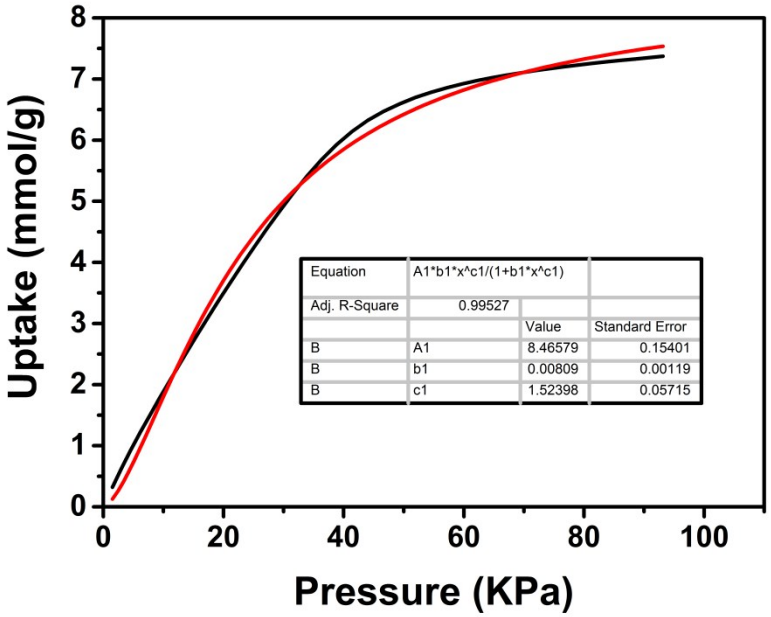

Figure S31. UPC-104: the parameters and optimized adsorption isotherms of n-C_4H_{10} for calculated selectivity by using Ideal Adsorbed Solution Theory (IAST) at 298K.

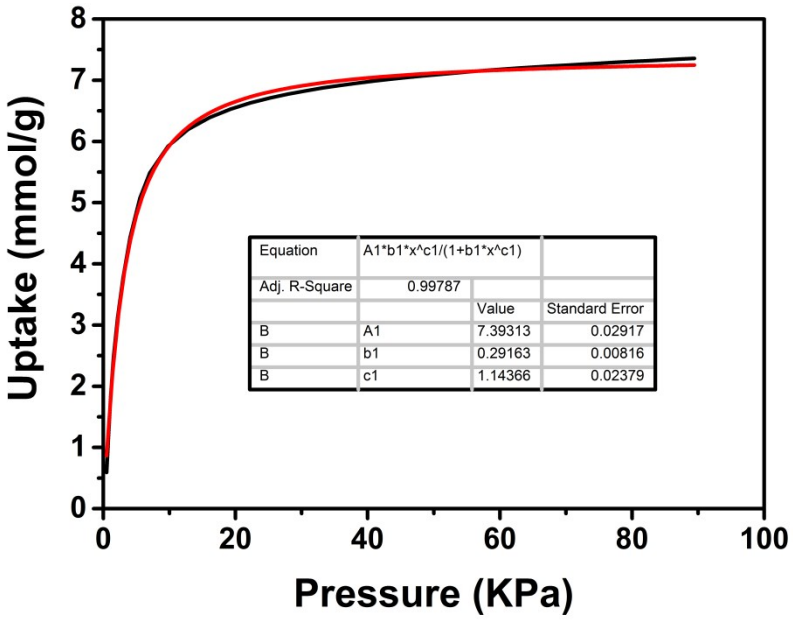

Figure S32. UPC-104: the parameters and optimized adsorption isotherms of i-C_4H_{10} for calculated selectivity by using Ideal Adsorbed Solution Theory (IAST) at 298K.

4. Computational methods

Density Functional Theory (DFT) Calculations: DFT calculations were performed to provide the optimized structures and energies of acetylene and propylene interaction with the frameworks of **UPC-104**. We used the Perdew–Burke–Ernzerhof (PBE)[73] functional under the generalized gradient approximation (GGA) functional with the double-ξ numerical polarization (DNP) basis set implemented in the DMol^3 program package in the Materials Studio of Accelrys Inc for our calculations. Since calculations using the whole unit cells are too large, we used fragmented cluster models cleaved from the unit cells for modeling the partial charges, structures, and energies. The cleaved bonds at the boundaries of the clusters were saturated by protons (Fig. S30). The tolerances of energy, gradient and displacement convergence were 1×10^{-5}

hartree, 2×10^{-3} hartree/Å, and 5×10^{-3} Å, respectively. The adsorption energies (ΔE_{ad})[74] of C_3H_6 and C_2H_2 molecules with the framework cluster of **UPC-104** were calculated by $E_{ad} = E_{gas} + E_{cluster} - E_{gas\text{-}cluster}$, where E_{gas}, $E_{cluster}$, and $E_{gas\text{-}cluster}$ are the total energies of the gas molecule, the fragmented cluster, and the adsorption system at their optimized geometries, respectively.

Grand Canonical Monte Carlo (GCMC) Calculations: In this work, the GCMC calculations,[75] which were performed by Sorption code embedded in the Material Studio (MS) software, were carried out to study the C_3H_6 adsorption capacity of **UPC-104** at given adsorption 298 K and 5 kPa. Periodic boundary conditions were applied in three dimensions. In addition, the Dreiding force field,[76] which was a purely diagonal force field with harmonic valence terms and a cosine-Fourier expansion torsion term, was used to describe the interatomic interaction. Specifically, the van der Waals interactions with a cutoff of 8 Å were depicted by the Lennard−Jones potential and the electrostatic interactions were described via atomic monopoles and a screened (distance-dependent) Coulombic term.

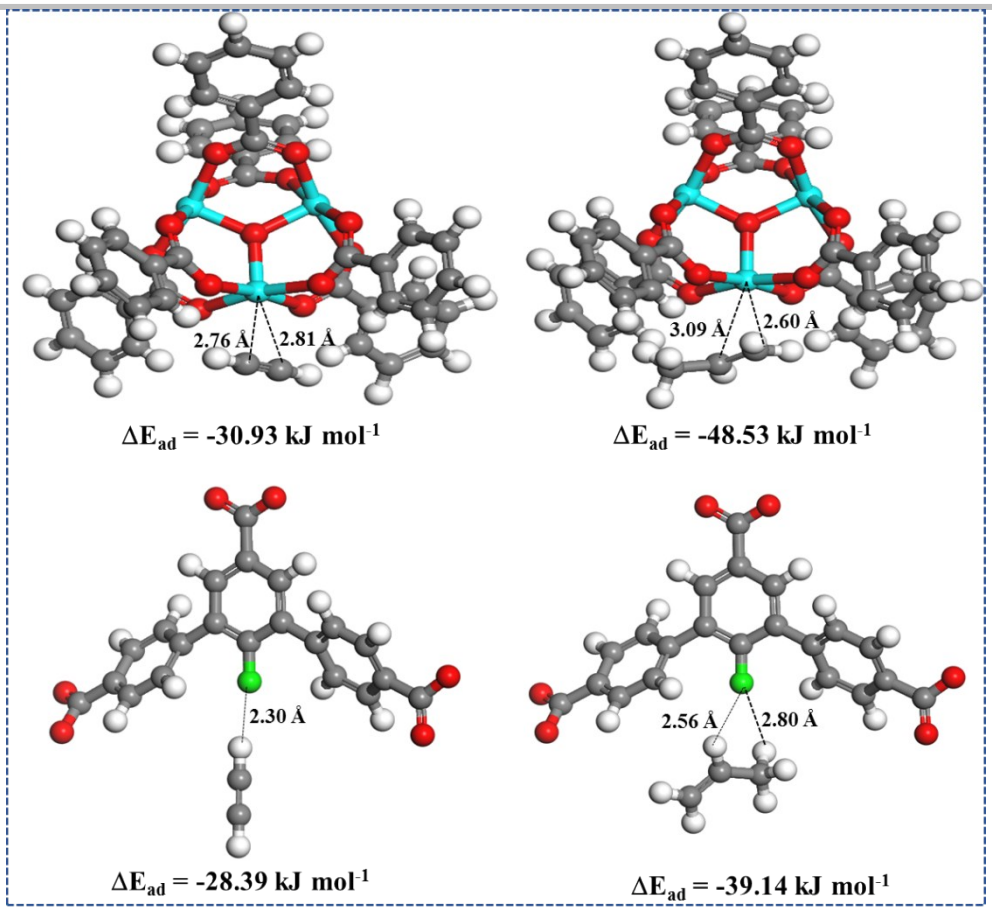

Fig. S33 Preferential C_2H_2 and C_3H_6 adsorption sites and corresponding adsorption energies in **UPC-104** obtained from first-principles calculations.

References

1. J. Shang, N. M. Gallagher, F. S. Bie, Q. L. Li, Y. K. Che, Y. Wang, and H. Jiang, J. Org. Chem. 2014, 79, 5134.
2. I. A. Ibarra, S. Yang, X. Lin, A. J. Blake, P. J. Rizkallah, H. Nowell, D. R. Allan, N. R. Champness and P. Hubberstey, Chem. Commun., 2011, 47, 8304.
3. S. M. Humphrey, J.-S. Chang, S. H. Jhung, J. W. Yoon and P. T. Wood, Angew. Chem., Int. Ed. 2007, 46, 272.
4. Y.-G. Lee, H. R. Moon, Y. E. Cheon and M. P. Suh, Angew. Chem., Int. Ed. 2008, 47, 7741.
5. H. J. Park, M. P. Suh, Chem.—Eur. J. 2008, 14, 8812.
6. K. S. Park, Z. Ni, A. P. Cote, J. Y. Choi, R. Huang, F. J. UribeRomo, H. K. Chae, M. O'Keeffe and O. M. Yaghi, Proc. Natl. Acad. Sci. U.S.A. 2006, 103, 10186.
7. Y.-G. Lee, H. R. Moon, Y. E. Cheon and M. P. Suh, Angew. Chem., Int. Ed. 2008, 47, 7741.
8. S. Barman, H. Furukawa, O. Blacque, K. Venkatesan, O. M. Yaghi and H. Berke, Chem. Commun., 2010, 46, 7981.
9. J. L. C. Rowsell, A. R. Millward, K. S. Park and O. M. Yaghi, J. Am. Chem. Soc., 2004, 126, 5666.
10. J. L. C. Rowsell, O. M. Yaghi, J. Am. Chem. Soc., 2006, 128, 1304.
11. Y. E. Lee, S. Y. Jang and M. P. Suh, J. Am. Chem. Soc., 2005, 127, 6374.
12. H. J. Park, D.-W. Lim, W. S. Yang, T.-R. Oh and M. P. Suh, Chem.—Eur. J. 2011, 17, 7251.
13. D. Han, F.-L. Jiang, M.-Y. Wu, L. Chen, Q.-X. Chen and M.-C. Hong, Chem. Commun., 2011, 47, 9861.
14. K. Sumida, C. M. Brown, Z. R. Herm, S. Chavan, S. Bordiga and J. R. Long, Chem. Commun., 2011, 47, 1157.
15. S. Ma, H.-C. Zhou, J. Am. Chem. Soc. 2006, 128, 11734.
16. D. Sun, S. Ma, Y. Ke, D. J. Collins and H.-C. Zhou, J. Am. Chem. Soc., 2006, 128, 3896.
17. H.-C. Zhou, S. Q. Ma, D. F. Sun, M. Ambrogio, J. A. Fillinger and S. Parkin, J. Am. Chem. Soc. 2007, 129, 1858.
18. A. G. Wong-Foy, O. Lebel and A. J. Matzger, J. Am. Chem. Soc. 2007, 129, 15740.
19. M. Kramer, U. Schwarz, S. Kaskel, J. Mater. Chem. 2006, 16, 2245.
20. W. Zhuang, S. Ma, X.-S. Wang, D. Yuan, J.-R. Li, D. Zhao and H.-C. Zhou, Chem. Commun. 2010, 46, 5223.
21. D. Zhao, D. Yuan, A. Yakovenko, H.-C. Zhou, Chem. Commun. 2010, 46, 4196.
22. T. K. Kim, M. P. Suh, Chem. Commun. 2011, 47, 4258.
23. T. K. Prasad, D. H. Hong, M. P. Suh, Chem.—Eur. J. 2010, 16, 14043.
24. D. Yuan, D. Zhao, D. Sun, H.-C. Zhou, Angew. Chem., Int. Ed. 2010, 49, 5357.
25. Y. Yan, S. Yang, A. J. Blake, W. Lewis, E. Poirier, S. A. Barnett, N. R. Champness and M. Schr€oder, Chem. Commun. 2011, 47, 9995.
26. D. Yuan, D. Zhao, H.-C. Zhou, Inorg. Chem. 2011, 50, 10528–10530.
27. O. K. Farha, A. O. Yazaydin, I. Eryazici, C. D. Malliakas, B. G. Hauser, M. G. Kanatzidis, S. T. Nguyen, R. Q. Snurr and J. T. Hupp, Nat. Chem. 2010, 2, 944.
28. X. Duan, J. Cai, J. Yu, C. Wu, Y. Cui, Y. Yang and G. Qian, Microporous Mesoporous Mater., 2013, 181, 99−104.
29. K. Liu, B. Li, Y. Li, X. Li, F. Yang, G. Zeng, Y. Peng, Z. Zhang, G. Li, Z. Shi, S. Feng and Song, D. Chem. Commun., 2014, 50, 5031−5033.
30. H. M. Wen, H. Wang,; B. Li, Y Cui, H. Wang, G. Qian and Chen, B. Inorg. Chem., 2016, 55, 7214−7218.
31. Z. Chen, S. Xiang, D. Zhao and B. Chen, Cryst. Growth Des., 2009, 9, 5293−5296.
32. J. Duan, W. Jin and R. Krishna, Inorg. Chem., 2015, 54, 4279−4284.
33. F. Luo, C. Yan, L. Dang, R. Krishna, W. Zhou, H. Wu, X. Dong, Y. Han, T. L. Hu, M. O'Keeffe, L. Wang, M. Luo, R. B. Lin and B. Chen, J.Am. Chem. Soc., 2016, 138, 5678−5684.
34. H. Xu, Y. He, Z. Zhang, S. Xiang, J. Cai, Y. Cui, Yang, Y. Yang, G. Qian and B. Chen, J. Mater. Chem. A., 2013, 1, 77−81.
35. M. Fischer, F. Hoffmann and M. Froba, ChemPhysChem 2010, 11, 2220−2229.
36. C. Song, J. Hu, Y. Ling, Y. Feng, D. L. Chen and Y. He, Dalton Trans. 2015, 44, 14823−14829.

37. Y. Ling, J. Jiao, M. Zhang, H. Liu, D. Bai, Y. Feng and Y. He, CrystEngComm., 2016, 18, 6254-6261.
38. G. Chang, B. Li, H. Wang, T. Hu, Z. Bao and B. Chen, Chem. Commun., 2016, 52, 3494−3496.
39. L. Zhang, C. Zou, M. Zhao, K. Jiang, R. Lin, Y. He, C.-D. Wu, Y. Cui, B. Chen and G. Qian, Cryst. Growth Des., 2016, 16, 7194.
40. X. Duan, R. Song, J. Yu, H. Wang, Y. Cui, Y. Yang, B. Chen and G. Qian, RSC Adv., 2014, 4, 36419−36424.
41. G. Chen,; Z. Zhang, S. Xiang and B. Chen, CrystEngComm., 2013, 15, 5232−5235.
42. Z. Zhang, S. Xiang, K. Hong, M. C. Das, H. D. Arman, Garcia, M. Garcia, J. U. Mondal, K. M. Thomas and B. Chen, Inorg. Chem., 2012, 51, 4947−4953.
43. L. Li,; X. Wang, J. Liang, Y. Huang, H. Li, Z. Lin and R. Cao, ACS Appl. Mater. Interfaces 2016, 8, 9777−9781.
44. H. Alawisi, B. Li, Y. He, H. D. Arman, A. M. Asiri, H. Wang and B. Chen, Cryst. Growth Des., 2014, 14, 2522–2526.
45. X. Duan, H. Wang, Z. Ji, Y. Cui, Y. Yang and G. Qian, J. Solid State Chem., 2016, 241, 152−156.
46. Y. Huang, Z. Lin, H. Fu, F. Wang, M. Shen, X. Wang and R. Cao, ChemSusChem, 2014, 7, 2647−2653.
47. Z. J. Guo, J. M. Yu, Y.Z. Zhang, J. Zhang, Y. Chen, Y. F. Wu, L. H. Xie and J. R. Li, Inorg. Chem., 2017, 56, 2188–2197.
48. R. Matsuda, R. Kitaura, S. Kitagawa, Y. Kubota, R. V. Belosludov, T. C. Kobayashi, H. Sakamoto, T. Chiba, M. Takata, Y. Kawazoe and Y. Mita, Nature, 2005, 436, 238–241.
49. D. G. Samsonenko, H. Kim, Y. Sun, G.-H. Kim, H.-S. Lee and K. Kim, Chem.–Asian J., 2007, 2, 484–488.
50. D. Tanaka, M. Higuchi, S. Horike, R. Matsuda, Y. Kinoshita, N. Yanai and S. Kitagawa, Chem.–Asian J., 2008, 3, 1343–1349.
51. J.-P. Zhang and S. Kitagawa, J. Am. Chem. Soc., 2008, 130, 907–917.
52. J.-P. Zhang and X.-M. Chen, J. Am. Chem. Soc., 2009, 131, 5516–5521.
53. S. Xiang, W. Zhou, J. M. Gallegos, Y. Liu and B. Chen, J. Am. Chem. Soc., 2009, 131, 12415–12419.
54. S. Xiang, W. Zhou, Z. Zhang, M. A. Green, Y. Liu and B. Chen, Angew. Chem., Int. Ed., 2010, 49, 4615–4618.
55. E. D. Bloch, W. L. Queen, R. Krishna, J. M. Zadrozny, C. M. Brown and J. R. Long, Science, 2012, 335, 1606–1610.
56. Y. He, R. Krishna and B. Chen, Energy Environ. Sci., 2012, 5, 9107–9120.
57. Y. He, Z. Zhang, S. Xiang, F. R. Fronczek, R. Krishna and B. Chen, Chem.–Eur. J., 2012, 18, 613–619.
58. Y. He, Z. Zhang, S. Xiang, H. Wu, F. R. Fronczek, W. Zhou,R. Krishna, M. O'Keeffe and B. Chen, Chem.–Eur. J., 2012, 18,1901–1904.
59. (a) Y. He, Z. Zhang, S. Xiang, F. R. Fronczek, R. Krishna and B. Chen, Chem. Commun., 2012, 48, 6493–6495; (b) Y. He, S. Xiang, Z. Zhang, S. Xiong, F. R. Fronczek, R. Krishna, M. O'Keeffee and B. Chen, Chem. Commun., 2012, 48, 10856–10858.
60. M. C. Das, H. Xu, S. Xiang, Z. Zhang, H. D. Arman, G. Qian and B. Chen, Chem.–Eur. J., 2011, 17, 7817–7822.
61. M. C. Das, H. Xu, Z. Wang, G. Srinivas, W. Zhou, Y.-F. Yue, V. N. Nesterov, G. Qian and B. Chen, Chem. Commun., 2011, 47, 11715–11717.
62. Y. Hu, S. Xiang, W. Zhang, Z. Zhang, L. Wang, J. Bai and B. Chen, Chem. Commun., 2009, 7551–7553.
63. Z. Zhang, S. Xiang, Y.-S. Chen, S. M. Lee, T. Phely-Bobin and B. Chen, Inorg. Chem., 2010, 49, 8444–8448.
64. Z. Zhang, S. Xiang, X. Rao, Q. Zheng, F. R. Fronczek, G. Qian and B. Chen, Chem. Commun., 2010, 46, 7205–7207.
65. Z. Chen, S. Xiang, H. D. Arman, J. U. Mondal, P. Li, D. Zhao and B. Chen, Inorg. Chem., 2011, 50, 3442–3446.
66. Z. Chen, S. Xiang, H. D. Arman, P. Li, S. Tidrow, D. Zhao and B. Chen, Eur. J. Inorg. Chem., 2010, 3745–3749.
67. Y. -S. Xue, Y. He, S. -B. Ren, Y. Yue, L. Zhou, Y. -Z. Li, H. -B. Du, X. -Z. You and B. Chen, J. Mater. Chem., 2012, 22, 10195–10199.

68. Z. Guo, H. Xu, S. Su, J. Cai, S. Dang, S. Xiang, G. Qian, H. Zhang, M. O'Keeffe and B. Chen, Chem. Commun., 2011, 47, 5551–5553.
69. P. Li, Y. He, Y. Zhao, L. Weng, H. Wang, R. Krishna, H. Wu, W. Zhou, M. O'Keeffe, Y. Han and B. A Chen, Angew. Chem., Int. Ed., 2014, 54, 574–577.
70. M. H. Zhang, X. L. Xin, Z. Y. Xiao, R. M. Wang, L. L. Zhang, D. F. Sun, J. Mater. Chem. A, 2017, 5, 1168–1175.
71. W. D. Fan, Y. T. Wang, Q. Zhang, A. Kirchon, Z. Y. Xiao, L. L. Zhang, F. N. Dai, R. M. Wang, D. F. Sun, Chem. Eur. J. 2018, 24, 2137–2143.
72. W. D. Fan, Y. T. Wang, Z. Y. Xiao, L. L. Zhang, Y. Q. Gong, F. N. Dai, R. M. Wang, D. F. Sun, Inorg. Chem. 2017, 56, 13634−13637.
73. Perdew, J. P.; Burke, K.; Ernzerhof, M. Generalized Gradient Approximation Made Simple. Phys. Rev. Lett. 1996, 77, 3865.
74. Grosjean, B.; Pean, C.; Siria, A.; Bocquet, L.; Vuilleumier, R.; Bocquet, M. Chemisorption of Hydroxide on 2D Materials from DFT Calculations: Graphene versus Hexagonal Boron Nitride. J. Phys. Chem. Lett. 2016, 7, 4695.
75. Li, X.; Jin, Y.; Xue, Q.; Zhu, L.; Xing, W.; Zheng, H.; Liu, Z. Ultra-High Selective Capture of CO_2 on One-sided N-doped Carbon Nanoscrolls. J. CO_2 Util. 2017, 18, 275−282.
76. Mayo, S. L.; Olafson, B. D.; Goddard, W. A. DREIDING: A Generic Force Field for Molecular Simulations. J. Phys. Chem. 1990, 94, 8897−8909.